Wide-Sense Nonblocking Conditions for Flex-Grid OXC-Clos Networks

Yibei Yao, Tong Ye, *Member, IEEE*, and Ning Deng, *Senior Member, IEEE*

***Abstract*— The emerging high-capacity optical networks make it urgent to design large-scale flexible mesh optical cross-connect (OXC). Though Clos networks are the theory for building scalable and cost-effective switching fabrics, the nonblocking conditions for flex-grid optical Clos networks without wavelength conversion remain unknown. This paper studies the nonblocking conditions for the flex-grid OXC-Clos network, which is constructed from a number of small-size standard OXCs. We first show that a strictly nonblocking (SNB) OXC-Clos network will incur a high cost, as small-granularity lightpaths may abuse central modules (CMs), rendering them unavailable for large-granularity requests due to frequency conflicts. Hence, we propose a granularity differential routing (GDR) strategy, the idea of which is to restrict the set of CMs that can be utilized by the lightpaths of each granularity. Under the GDR strategy, we investigate two system models, called granularity-port binding and unbinding models, and prove the wide-sense nonblocking (WSNB) conditions. We show that the cost of WSNB network is remarkably smaller than that of SNB network, and find that the granularity-port unbinding model can offer more flexible network-bandwidth utilization compared to the binding model, with a slight cost associated with switching fabrics.**

***Index Terms*— Optical cross-connect, flex-grid optical network, wide-sense nonblocking, strictly nonblocking.**

I. Introduction

IN RECENT years, the surge in Internet traffic caused by high-performance computing services and multimedia services is driving the continuous growth of optical network capacity. On one hand, the bandwidth of single-fiber links will be exhausted and the use of multiple fibers on optical links has been put on the agenda. As Ref. [1] points out, optical fiber deployment is growing at an annual rate of 15%. On the other hand, the data rates of signals launched into the optical links climb up from 10 Gb/s to 100 Gb/s, and will soon reach 400 Gb/s and above. It is necessary to maximize spectral efficiency according to the data rate and the transmission distance of each demand [2]. In this context, the traditional fixed-grid optical networks, which divide the optical spectrum into fixed wavelength grids, are becoming inefficient.

Received 2 April 2024; revised 11 September 2024; accepted 9 December 2024. Date of publication 25 February 2025; date of current version 14 May 2025. This work was supported by the National Science Foundation of China (NSFC) under Grant 62271306 and Grant 62331017. An earlier version of this paper was presented in part at the IEEE INFOCOM 2024 [DOI: 10.1109/INFOCOM52122.2024.10621334]. *(Corresponding author: Tong Ye.)*

Yibei Yao and Tong Ye are with the State Key Laboratory of Photonics and Communications, Shanghai Jiao Tong University, Shanghai 200240, China (e-mail: yaoyibei@sjtu.edu.cn; yetong@sjtu.edu.cn).

Ning Deng is with the School of Computing and Information Technology, Great Bay University, Guangdong 523000, China (e-mail: ndeng@gbu.edu.cn).

Digital Object Identifier 10.1109/JSAC.2025.3543546

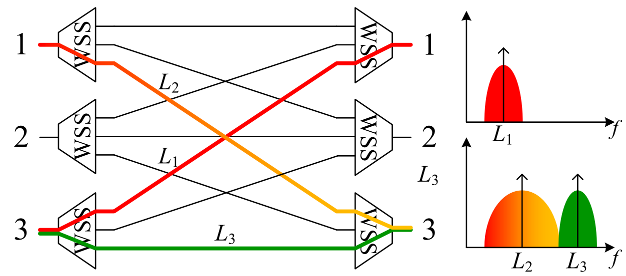

Fig. 1. A standard 3×3 OXC, where L_i stands for lightpath i and different colors represent different optical frequencies.

In contrast, the flex-grid optical network, also called elastic optical network (EON) [3], [4], [5], [6], [7], is emerging to support lightpaths of different bandwidths. Accordingly, the design of optical network components should adapt to the new changes.

In the meanwhile, optical cross-connect (OXC) has become the key component of switching nodes in optical networks. As Fig. 1 shows, a classical $N \times N$ OXC includes N $1 \times N$ wavelength selective switches (WSSs) at the input side and N $N \times 1$ WSSs at the output side, with an $N^2 \times N^2$ shuffle interconnection network in between. The OXC is a flexible optical switching fabric. If there is a common spectrum interval free on an input and an output, the OXC can establish a lightpath in a strictly nonblocking (SNB) manner. Fig. 1 displays three lightpaths occupying different spectral bandwidths. However, the scalability of classical OXC is restricted by the WSS, the port count of which is currently limited to 49 [8]. The classical OXC cannot meet the application requirement of future optical networks, which will require optical nodes with hundreds of ports due to the use of multiple fibers on each optical link. Thus, it is highly desired to enhance the scalability of OXCs.

Clos network is the theory to construct a scalable and cost-effective switching fabric. In the past decades, different electrical/optical Clos switches [9], [10], [11], [12], [13], [14] and the related nonblocking conditions have been studied. However, only a few endeavors have been made to apply this theory to construct scalable flex-grid OXCs, called flex-grid OXC-Clos network in this paper, whose nonblocking conditions are still unknown.

This paper only considers the flex-grid OXC-Clos network without wavelength converters (WCs), since all-optical WCs are not commercially available in the current stage. In a flex-grid OXC-Clos network without WCs, each lightpath must use a common and continuous optical spectrum on all the internal links of the switching fabric, in addition to the input and the output. As Section VII will state, this feature is quite different from that of multi-rate Clos networks studied in the 1990s, which allow a connection to use different and discontinuous spectral segments on internal links. Thus, the approaches and the results of multi-rate Clos networks [12], [15], [16], [17], [18] cannot be applied to the flex-grid OXC-Clos networks.

This paper pursues the nonblocking conditions of flex-grid OXC-Clos networks, since nonblocking switching nodes can simplify the routing and spectrum allocation (RSA) of optical networks. In an optical network with nonblocking switching nodes, an end-to-end lightpath can be established, as long as a common and continuous spectrum can be found on all the links along a path from the source to the destination. In other words, when performing RSA, it is unnecessary for the optical network to consider the internal state of switching nodes.

In addition to nonblocking conditions, we emphasize on the ability of flex-grid OXC-Clos networks to establish lightpaths without any reconfiguration. Such an ability is of great significance for industrial applications, because the reconfiguration means the interruption of ongoing services provided by the existing lightpaths. SNB and wide-sense nonblocking (WSNB) switching networks are designed to offer this switching ability. An SNB network can always build a new connection without any reconfiguration, while a WSNB network can do that with the help of a specific routing strategy.

The major contribution of this paper is to devise a granularity differential routing (GDR) strategy, and seek the WSNB conditions for flex-grid OXC-Clos networks. Our proposal is motivated by the derivation of the SNB condition for flex-grid OXC-Clos networks. We show that the small-granularity lightpaths in an SNB OXC-Clos network will probably lead to excessive occupation of central modules (CMs), which become unavailable for future large-granularity requests due to spectral conflicts. As a result, a lot of CMs are needed by an SNB flex-grid OXC-Clos network. The key idea of our GDR strategy is to restrict the set of CMs that can be used by the lightpaths of each granularity, thereby leaving more CMs for subsequent large-granularity requests. Under the GDR strategy, we prove the WSNB conditions for flex-grid OXC-Clos network and show that the number of CMs needed by a WSNB OXC-Clos network is remarkably smaller than that by an SNB network. Also, the GDR strategy does not require any calculation, and thus almost does not increase operation complexity.

In this paper, we consider two application models under the flex-grid scenario, when deriving WSNB conditions. The first one, named granularity-port binding (GPB) model, stems from a practical application scenario, where each port of the optical switch only carries the lightpaths with the same granularity. The second one, entitled granularity-port unbinding (GPuB) model, allows the lightpaths of different granularities to coexist in a port of the switching fabric. Compared to the GPB model, the GPuB model has more flexibility in port utilization. We show that the sufficient WSNB condition for the GPB model is the necessary and sufficient WSNB condition for the GPuB model, indicating that flexibly deploying lightpaths among the ports only leads to a slightly higher cost.

The rest of this paper is organized as follows. In Section II, we introduce the OXC-Clos network, define two patterns of lightpath granularity and two application models, and analyze the cost of SNB networks. According to the analysis, Sections III and IV propose the GDR strategy and derive the WSNB conditions under the GPB model and the GPuB model, respectively, when the granularity pattern is exponential. Section V further checks the effectiveness of the GDR strategy when the granularity pattern is linear. Section VI shows how a WSNB OXC-Clos network can be applied to the multi-fiber flex-grid networks. Section VII reviews the related works and makes a comparison between the WSNB OXC-Clos network and some previously proposed OXC structures. Section VIII concludes this paper.

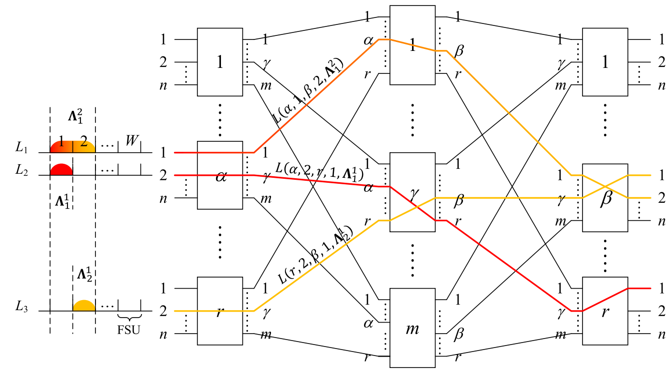

Fig. 2. A flex-grid optical Clos Network $\mathcal{C}(n,r,m)$ with 3 lightpaths.

II. PRELIMINARY

As Fig. 2 displays, an $N\times N$ symmetric flex-grid OXC-Clos network, denoted by $\mathcal{C}(n,r,m)$, includes r $n\times m$ input modules (IMs) at the input stage, m $r\times r$ central modules (CMs) at the central stage, and r $m\times n$ output modules (OMs) at the output stage, where $N=n\times r$. Each module in $\mathcal{C}$ is a small-scale standard OXC, as the one shown in Fig. 1. Hence, each module in OXC-Clos networks is called OXC module in this paper. The two OXC modules at the adjacent stages are connected by a single fiber. From top to bottom, we number the IMs by $1,\cdots,\alpha,\cdots,r$, the CMs by $1,\cdots,\gamma,\cdots,m$, and the OMs by $1,\cdots,\beta,\cdots,r$. Similarly, we number the inputs of each IM as $1,\cdots,a,\cdots,n$, and the outputs of each OM as $1,\cdots,b,\cdots,n$.

In a flex-grid optical network, the spectrum of each port is divided into W frequency slot units (FSUs), the width of which is 12.5 GHz [19]. In Fig. 2, an FSU is represented by a slot. We number W FSUs by $1,\cdots,w,\cdots,W$. A set of ω adjacent FSUs indexed by $w,w+1,\cdots,w+\omega-1$ defines an ω-granularity (ω-g) frequency slot, which is denoted by $\mathbf{\Lambda}_w^\omega$ in this paper, where w and ω are two positive integers and $w+\omega-1\leq W$. The "flex-grid" means that the frequency slots with different granularities can coexist in the network.

This paper considers the communication mode, in which the network sets up an ω-g lightpath from an input to an output if there is a frequency slot $\mathbf{\Lambda}_w^\omega$ free on them. We denote an ω-g lightpath from input a of IM α to output b of OM β as $L(\alpha,a,\beta,b,\mathbf{\Lambda}_w^\omega)$. Similarly, a lightpath request is denoted by $R(\alpha,a,\beta,b,\mathbf{\Lambda}_w^\omega)$. For example, L_1 in Fig. 2 is a 2-g lightpath, denoted by $L\left(\alpha,1,\beta,2,\mathbf{\Lambda}_1^2\right)$, and L_2 and L_3 are two 1-g lightpaths, denoted by $L\left(\alpha,2,r,1,\mathbf{\Lambda}_1^1\right)$ and $L\left(r,2,\beta,1,\mathbf{\Lambda}_2^1\right)$. Also, the spectrum interval used by a lightpath is represented by a colored box covering several slots in the figure. As an instance, the spectrum interval of L_1 includes FSUs 1 and 2.

The OXC-Clos network has two routing constraints. That is, two lightpaths cannot use the same CM, if

C1. They share the same IM and occupy the same FSUs, or
C2. They share the same OM and occupy the same FSUs.

The example for constraint C1 is L_1 and L_2 in Fig. 2 and that for C2 is L_1 and L_3 in Fig. 2.

Definition 1: An OXC is SNB if a lightpath can always be set up between an input and an output without rearranging the paths of the existing lightpaths when the input and output have the same idle spectrum interval.

Definition 2: An OXC is WSNB if a routing strategy exists for setting lightpaths in such a way that a lightpath can always be set up between an input and an output without rearranging the paths of the existing lightpaths when the input and output have the same idle spectrum interval.

Please note that $\mathcal{C}$ reduces to a classical OXC when $n = 1$, and the CMs in $\mathcal{C}$ change to m fiber lines, when $r = 1$. Thus, this paper only considers the case where $n, r > 1$.

A. System Models

To facilitate our theoretical study, we assume that there are K types of lightpaths (or frequency slots) in the network and

A1. There are $W = 2^{K-1}$ FSUs,
A2. The k-th type of lightpath occupies 2^{k-1} adjacent FSUs, where $k = 1, 2, \cdots, K$.

We refer to such a kind of granularity pattern as exponential granularity pattern. **Note that** the idea of our approach in this paper is not limited to the exponential granularity pattern presented in A2 and can be applied to other kinds of granularity patterns, as Section VI will show.

Also, we consider two models in this paper.

M1. **Granularity-Port Binding (GPB) model**: Once a port is used by a type of lightpaths, this port can only carry this type of lightpaths until it becomes completely free, which means all the lightpaths on this port are torn down.

Fig. 3(a) displays a 3×3 OXC, each port of which carries 8 FSUs. Input 1 only carries 2-g lightpaths once it is occupied by a 2-g lightpath. If input 1 becomes completely idle after all the 2-g lightpaths are torn down, it can be rebound by other types of lightpaths.

The GPB model stems from practical applications. There is one type of most cost-effective transceiver, when building an optical network. It is a common practice in real networks to adopt one modulation format with one granularity, which can simplify network management and maintenance. Hence, the single-fiber network typically has only one granularity of optical signals. When the network is upgraded by installing more fibers, a different type of transceiver with another granularity may likely be added to match the newly installed fibers. In this case, the flex-grid optical network will be possibly deployed according to the GPB model in the near future.

To avoid bandwidth fragmentation and maximize bandwidth utilization under the GPB model, this paper makes the following restriction:

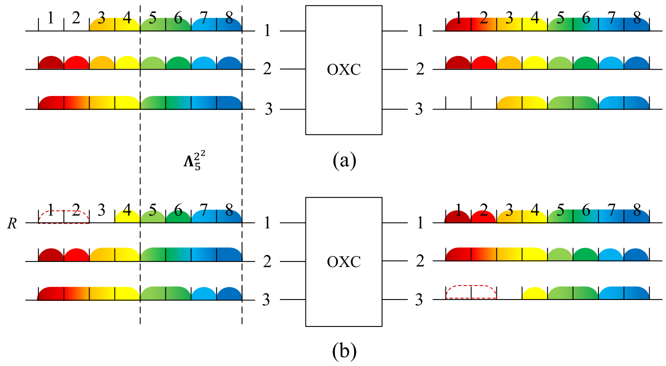

Fig. 3. Examples of (a) GPB model and (b) GPuB model, where $N = 3$, $K = 4$, and request R is represented by a dotted box.

A3. A 2^k-g lightpath is carried by a 2^k-g frequency slot, and the i-th 2^k-g frequency slot is defined by the set

$$\mathbf{\Lambda}_{2^k(i-1)+1}^{2^k} = \left\{2^k(i-1)+1, \cdots, 2^k i\right\}.$$

For example, $\mathbf{\Lambda}_5^{2^2} = \{5, 6, 7, 8\}$ in Fig. 3(a) defines the second 2^2-g frequency slot, while FSUs 3 through 6 do not form a 2^2-g frequency slot. The violation of A3 may lead to bandwidth fragmentation. Consider the following case. If input 3 in Fig. 3(a) carries a 2^2-g lightpath using FSUs 3 through 6, FSUs 1, 2, 7, and 8 will be wasted under the GPB model until this input becomes completely idle.

A3 implies that a 2^k-g frequency slot can accommodate up to 2^{k-i} 2^i-g lightpaths or be completely occupied by a 2^j-g lightpath, where $0 \le i < k < j \le K - 1$. For example, FSUs 5 and 6 in Fig. 3(a) form a 2^1-g frequency slot $\mathbf{\Lambda}_5^2$. $\mathbf{\Lambda}_5^2$ at the second input carries 2 1-g lightpaths, while that at the third input is used by one 2^2-g lightpath.

We notice that the flex-grid networks have just been built for less than 10 years. As traffic increases, the optical network will undergo multiple upgrades. In this case, the GPB model may lead to an inflexible utilization of network-link capacity. For example, although input 1 in Fig. 3(a) has two free FSUs, it cannot offer bandwidth to a 1-g request due to granularity-port binding. Allowing multiple granularities coexisting in the same fiber would be a better choice. We thus slightly relax the constraint imposed by granularity-port binding and explore a more flexible model as follows.

M2. **Granularity-Port unBinding (GPuB) model**: Each port can carry different types of lightpaths.

The "*slightly relax*" means we still consider A3 in the GPuB model. Fig. 3(b) illustrates the GPuB model, where input 1 has 3 idle FSUs. As A3 specifies, if a 2-g request from input 1 to output 3 arrives, input 1 will allocate FSUs 1 and 2 to this request, instead of FSUs 2 and 3.

B. Cost of SNB Flex-Grid Clos Network

The SNB condition for traditional Clos networks, i.e., $m \ge 2n-1$ [9], cannot be applied to flex-grid OXC-Clos Networks. Fig. 4 is an OXC-Clos network $\mathcal{C}(2, 2, 3)$, where there are three lightpaths and $m \ge 2n - 1 = 3$. However, as Fig. 4 plots, $R(1, 2, 1, 2, \mathbf{\Lambda}_1^2)$ is blocked, since lightpaths L_1 and L_2 share the same IM with R and use CMs 1 and 3 while lightpath L_3 shares the same OM with R and passes through CM 2.

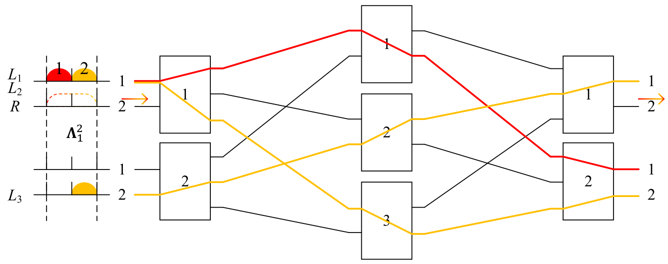

Fig. 4. Flex-grid OXC-Clos Network $\mathcal{C}(2,2,3)$ is not SNB, where request R is represented by a dotted box.

No CM is available for R due to frequency conflicts. In fact, the number of CMs needed by an SNB flexible OXC-Clos is very large, as we show in the following theorem.

Theorem 1: When K types of lightpaths coexist, $\mathcal{C}(n,r,m)$ is SNB iff

$$m \geq 2^K(n-1)+1. \tag{1}$$

Proof: Suppose there is a request $R\left(\alpha,a,\beta,b,\boldsymbol{\Lambda}_1^{2^{K-1}}\right)$ from input a of IM α to output b of OM β. Consider the worst case, where frequency slot $\boldsymbol{\Lambda}_1^{2^{K-1}}$ is busy in carrying 2^{K-1} 1-g lightpaths on all other inputs of IM α and all other outputs of OM β.

Let $\boldsymbol{S}_\alpha$ and $\boldsymbol{S}_\beta$ be the set of CMs used by the 1-g lightpaths from IM α and that used by the 1-g lightpaths ahead to OM β, respectively. Clearly,

$$|\boldsymbol{S}_\alpha| \leq 2^{K-1}(n-1),$$

and

$$|\boldsymbol{S}_\beta| \leq 2^{K-1}(n-1),$$

where the equalities hold if each lightpath uses a separate CM. Also,

$$|\boldsymbol{S}_\alpha \cup \boldsymbol{S}_\beta| \leq |\boldsymbol{S}_\alpha| + |\boldsymbol{S}_\beta| = 2^K(n-1),$$

where the inequality holds with equality when $\boldsymbol{S}_\alpha \cap \boldsymbol{S}_\beta = \phi$.

According to routing constraints C1 and C2, request R can be satisfied only when there is at least one more CM that is not employed by the lightpaths that originate from IM α or the lightpaths that go to OM β. We thus need

$$m = 2^K(n-1)+1$$

CMs to accommodate R. □

Clearly, (1) immediately reduces to the SNB condition of traditional Clos network when $K=1$, i.e., there is only one type of lightpaths in the network.

Theorem 1 shows that the number of CMs required by an SNB flex-grid OXC-Clos network is large, which is attributed to the fact that small-granularity lightpaths (e.g., 1-g lightpaths) may abuse the CMs such that a large number of CMs will not be available for future large-granularity requests. As Fig. 4 plots, the two 1-g lightpaths L_1 and L_2 at input 1 of IM α use two different CMs, though they could potentially share the same CM since they utilize different FSUs. This motivates us to devise a routing strategy, which restricts the set of CMs occupied by small-granularity lightpaths.

III. WSNB Condition Under GPB Model

In this section, we will develop a routing strategy under the GPB model to restrict the set of CMs occupied by small-granularity lightpaths, such that the number of CMs needed by a nonblocking OXC-Clos network can be reduced. The key problem is to figure out the set of CMs that each type of lightpaths can employ for routing. We solve this problem in an inductive manner. Specifically, we first find the sets of CMs that can be used by 1-g lightpaths and 2-g lightpaths in section III-A and III-B, from which section III-C then proposes the GDR strategy and proves the WSNB condition.

A. CMs That 1-g Lightpaths Can Use

We first determine the minimal number of CMs required by $\mathcal{C}$ to route 1-g lightpaths without reconfiguration when all K types of lightpaths coexist. Based on this information, we specify the set of CMs, via which the 1-g lightpaths should be routed.

Definition 3: In the case where $\mathcal{C}$ needs to support K types of lightpaths, $\mathcal{C}$ is SNB for 2^k-g lightpaths if it can always satisfy a 2^k-g request $R\left(\alpha,a,\beta,b,\boldsymbol{\Lambda}_w^{2^k}\right)$ without reconfiguration as long as frequency slot $\boldsymbol{\Lambda}_w^{2^k}$ is available on both input a of IM α and output b of OM β, where w is the first FSU of a 2^k-g frequency slot and $k=0,1,\cdots,K-1$.

Consider an OXC-Clos network with a set of routed lightpaths and a newly arrived 1-g request $R\left(\alpha,a,\beta,b,\boldsymbol{\Lambda}_w^1\right)$. The granularity of each routed lightpaths is $1 \leq k \leq K$. Clearly, no matter what k is, $\boldsymbol{\Lambda}_w^1$ in each of the other $n-1$ inputs excluding input a on IM α can only be occupied by one k-g lightpath. Similar situation exists on OM β. It follows that, regardless of whether there are already lightpaths with a granularity larger than 1, an OXC-Clos network with $2n-1$ CMs can satisfy all the 1-g requests without any reconfiguration, as the following lemma states.

Lemma 1: $\mathcal{C}$ is SNB for 1-g lightpaths under the GPB model iff $m \geq 2n-1$.

Proof: Suppose there is a request $R\left(\alpha,a,\beta,b,\boldsymbol{\Lambda}_w^1\right)$. Consider the case, where

(a) All other $n-1$ inputs of IM α are busy carrying $n-1$ lightpaths, each of which occupies $\boldsymbol{\Lambda}_w^1$;
(b) All other $n-1$ outputs of OM β are busy carrying $n-1$ lightpaths, each of which occupies $\boldsymbol{\Lambda}_w^1$.

The granularity of the lightpaths carried by each port is the same and could be any of $1,2,\cdots$, or 2^{K-1}.

Let $\boldsymbol{S}_\alpha$ be the set of CMs used by the lightpaths that occupy $\boldsymbol{\Lambda}_w^1$ and originate from IM α, and $\boldsymbol{S}_\beta$ be the set of CMs used by the lightpaths that occupy $\boldsymbol{\Lambda}_w^1$ and head for OM β. Clearly, $|\boldsymbol{S}_\alpha| = |\boldsymbol{S}_\beta| = n-1$. Also,

$$|\boldsymbol{S}_\alpha \cup \boldsymbol{S}_\beta| \leq |\boldsymbol{S}_\alpha| + |\boldsymbol{S}_\beta| = 2(n-1),$$

where the inequality holds with equality when $\boldsymbol{S}_\alpha \cap \boldsymbol{S}_\beta = \phi$.

According to constraints C1 and C2, R can be satisfied only if there is at least one CM that is not used by the lightpaths mentioned in (a) and (b). We thus need

$$m = 2n-1$$

CMs to accommodate R, which proves this lemma. □

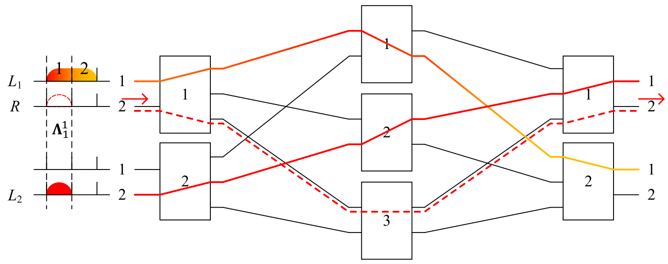

Fig. 5. $\mathcal{C}(2,2,3)$ is SNB for 1-g lightpaths though it carries two types of lightpaths.

Lemma 1 is illustrated in Fig. 5, where 3 CMs are enough to satisfy a 1-g request R without any reconfiguration, though a 2-g lightpath L_1 and a 1-g lightpath L_2 are in the network.

B. CMs That 2-g Lightpaths Can Use

Consider a 2-g request $R(\alpha, a, \beta, b, \mathbf{\Lambda}_w^2)$ that arrives at an OXC-Clos network, where some lightpaths are already established. In the following, we demonstrate how the routing of R is influenced by the lightpaths of different granularities.

Assume that all existing lightpaths are 1-g lightpaths. On IM α, frequency slot $\mathbf{\Lambda}_w^2$ on the $n-1$ inputs other than input a can accommodate up to $2(n-1)$ lightpaths. This is true on OM β. If no restrictions are made for the 1-g lighpaths, the 1-g lightpaths can utilize up to $4(n-1)$ CMs, rendering them unavailable for request R.

Suppose that all existing lightpaths are 2-g lightpaths. On IM α, $\mathbf{\Lambda}_w^2$ on the $n-1$ inputs other than input a can at most carry $n-1$ lightpaths. Similarly, OM β can at most carry $n-1$ lightpaths, if all $n-1$ other outputs are busy. These lightpaths will block at most $2(n-1)$ CMs for the request.

At last, we check the case where the granularity of lightpaths is 2^k, where $2 \leq k \leq K$. On IM α, frequency slot $\mathbf{\Lambda}_w^2$ on $n-1$ inputs other than input a can be occupied by up to $n-1$ 2^k-g lightpaths. The situation is similar on OM β. These 2^k-g lightpaths with $k > 1$ will make at most $2(n-1)$ CMs unavailable for the request. In other words, the lightpaths with granularity larger than 2 in $\mathbf{\Lambda}_w^2$ do not lead to excessive CM utilization.

Fortunately, Lemma 1 allows restricting the routing of all 1-g lightpaths to $2n-1$ CMs, such that more CMs can be left for future 2-g requests under the condition that all the 1-g requests can be satisfied. We are ready to check the minimum number of CMs required to route 1-g lightpaths and 2-g lightpahts without any reconfiguration when there is a routing restriction for 1-g lightpaths as follows.

Routing Strategy for 1-g lightpaths:

1) Specify a fixed set of $2n-1$ CMs, denoted by $\boldsymbol{M}_0$, via which all 2^0-g lightpaths can only be routed;
2) Lightpaths with granularity larger than 2^0 can be routed via the set of all CMs, denoted by $\boldsymbol{M}$.

Herein, we specify $\boldsymbol{M}_0 = \{1, 2, \cdots, 2n-1\}$.

Definition 4: In the case where $\mathcal{C}$ needs to support K types of lightpaths, $\mathcal{C}$ is WSNB for 2^k lightpaths if it can always satisfy a 2^k-g request $R\left(\alpha, a, \beta, b, \mathbf{\Lambda}_w^{2^k}\right)$ without reconfiguration under a routing strategy as long as frequency slot $\mathbf{\Lambda}_w^{2^k}$ is free on both input a of IM α and output b of OM β, where w is the first FSU of a 2^k-g frequency slot and $k = 0, 1, \cdots, K-1$.

Before finding the minimal number of CMs required to route 1-g and 2-g lightpaths without reconfiguration when $\mathcal{C}$ has to support K types of lightpaths, we need the following lemma.

Lemma 2: $f(x) = x - \lceil x/2 + a \rceil$ is non-decreasing, where $x = 1, 2, \cdots$ and a is an integer constant.

Lemma 3: Under Routing Strategy for 1-g lightpaths, $\mathcal{C}$ is WSNB for both 1-g and 2-g lightpaths under the GPB model iff $m \geq 3n-2$.

Proof: Consider a request $R(\alpha, a, \beta, b, \mathbf{\Lambda}_w^2)$ that sees the following situation:

(a) p_α inputs of IM α and p_β outputs of OM β are busy carrying 1-g lightpaths via $\mathbf{\Lambda}_w^2$, and

(b) $n-p_\alpha-1$ inputs of IM α and $n-p_\beta-1$ outputs of OM β are busy carrying the last $K-1$ types of lightpaths via $\mathbf{\Lambda}_w^2$, and each port only carries one type of lightpaths,

where $p_\alpha, p_\beta = 0, 1, \cdots, n-1$.

Let $\boldsymbol{B}_0$ be the set of CMs used by the 1-g lightpaths that are carried by IM α or OM β via $\mathbf{\Lambda}_w^2$. According to lemma 1, all 1-g lightpaths can be routed via the CMs in $\boldsymbol{M}_0$, which means

$$|\boldsymbol{B}_0| \leq |\boldsymbol{M}_0| = 2n-1. \tag{2}$$

Let $\boldsymbol{S}_\alpha$ be the set of CMs used by the last $K-1$ types of lightpaths that occupy $\mathbf{\Lambda}_w^2$ and originate from IM α, and $\boldsymbol{S}_\beta$ be the set of CMs used by the last $K-1$ types of lightpaths that occupy $\mathbf{\Lambda}_w^2$ and head for OM β. Note that a lightpath with granularity larger than 1 uses all the FSUs in $\mathbf{\Lambda}_w^2$ and thus cannot share the same CM with another one that also occupies $\mathbf{\Lambda}_w^2$, if both of them originate from IM α or visit OM β. It follows that

$$|\boldsymbol{S}_\alpha| = n - p_\alpha - 1,$$
$$|\boldsymbol{S}_\beta| = n - p_\beta - 1,$$

and thus

$$|\boldsymbol{S}_\alpha \cup \boldsymbol{S}_\beta| \leq |\boldsymbol{S}_\alpha| + |\boldsymbol{S}_\beta| = 2(n-1) - (p_\alpha + p_\beta). \tag{3}$$

where the inequality holds with equality when $S_\alpha \cap S_\beta = \phi$.

$p_\alpha + p_\beta$ in (3) can be determined as follows. Any two 1-g lightpaths carried by p_α inputs of IM α or p_β outputs of OM β via $\mathbf{\Lambda}_w^2$ can share the same CM, as long as they do not use the same set of FSUs. This implies that $|\boldsymbol{B}_0|$ must be less or equal to the number of these lightpaths. Furthermore, the total number of FSUs in $\mathbf{\Lambda}_w^2$ on p_α inputs of IM α and p_β outputs of OM β is $2(p_\alpha + p_\beta)$, which can carry up to $2(p_\alpha + p_\beta)$ 1-g lightpaths. Thus, we have $|\boldsymbol{B}_0| \leq 2(p_\alpha + p_\beta)$ or

$$p_\alpha + p_\beta \geq \left\lceil \frac{|\boldsymbol{B}_0|}{2} \right\rceil. \tag{4}$$

It follows from (3) through (4) that the set of CMs that are not available for request R satisfies

$$\begin{aligned}
|\boldsymbol{B}_0 \cup \boldsymbol{S}_\alpha \cup \boldsymbol{S}_\beta| &\leq |\boldsymbol{B}_0| + |\boldsymbol{S}_\alpha \cup \boldsymbol{S}_\beta| \\
&\leq |\boldsymbol{B}_0| + 2(n-1) - (p_\alpha + p_\beta) \\
&\leq |\boldsymbol{B}_0| + 2(n-1) - \left\lceil \frac{|\boldsymbol{B}_0|}{2} \right\rceil \\
&\leq |\boldsymbol{M}_0| + 2n - 2 - \left\lceil \frac{|\boldsymbol{M}_0|}{2} \right\rceil \\
&= 2n - 1 + 2n - 2 - n \\
&= 3n - 3,
\end{aligned} \tag{5}$$

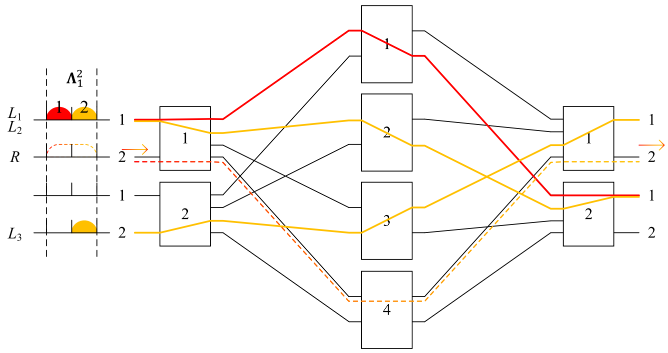

Fig. 6. $\mathcal{C}(2,2,4)$ is WSNB for 2^0-g and 2^1-g lightpaths, where $\boldsymbol{M}_0 = \{1,2,3\}$ and $\boldsymbol{M}_1 = \{1,2,3,4\}$.

where we use Lemma 2 and (2) for the fourth inequality. For an arbitrary $n \geq 2$, the inequality of (5) holds for equality if R sees the following situation when it arrives:

(i) In IM α, each of the $n-1$ inputs carries 2 2^0-g lightpath via $\boldsymbol{\Lambda}_w^2$, and

(ii) In OM β, one output carries 1 2^0-g lightpath via $\boldsymbol{\Lambda}_w^2$, and each of the other $n-2$ outputs carries 1 2^1-g lightpath via $\boldsymbol{\Lambda}_w^2$.

All the lightpaths in (i) and (ii) are different and use different CMs. In particular, $2n-1$ 2^0-g lightpaths are routed via CMs $1, 2, \cdots, 2n-1$, and $n-2$ 2^1-g lightpaths are routed via CMs $2n, 2n+1, \cdots, 3n-3$, which conforms with the GDR strategy. We thus need $m \geq 3n-2$ CMs to satisfy R. □

Lemma 3 implies the OXC-Clos network is WSNB for both 1-g and 2-g lightpaths, under the routing strategy as follows:

1) Specify a CM set $\boldsymbol{M}_0 = \{1, 2, \cdots, 2n-1\}$ for all 2^0-g lightpaths, via which 2^0-g lightpaths can only be routed;
2) Specify a CM set $\boldsymbol{M}_1 = \{1, 2, \cdots, 3n-2\}$ for all 2^1-g lightpaths, via which 2^1-g lightpaths can only be routed;
3) Lightpaths with granularity larger than 2^1 can be routed via the set of all CMs, denoted by $\boldsymbol{M}$.

Fig. 6 illustrates the routing strategy for 2^0-g and 2^1-g lightpaths in $\mathcal{C}(2,2,4)$, where the 2^0-g lightpaths L_1, L_2, and L_3 are routed via CMs 1, 2, 3, and the 2^1-g lightpaths can employ all the CMs.

C. GDR Strategy and WSNB Condition

We are now ready to consider the k-g request, where $2 \leq k \leq K$. Following the argument similar to that presented at the beginning of Section III-B, we need a routing strategy in this case to restrict the utilization of CMs by all the lightpaths with a granularity less than k. In this part, we generalize Lemmas 1 and 3 to propose the GDR strategy for K types of lightpaths, and we prove the WSNB condition for the flex-grid OXC-Clos network.

The **GDR Strategy** in general case is as follows:

1) Specify a set of CMs
$$\boldsymbol{M}_i = \{1, 2, \cdots, 2n-1+i(n-1)\}$$
for 2^i-g lightpaths, via which all the 2^i-g lightpaths can only be routed, where $i = 0, 1, \cdots, K-2$;
2) 2^{K-1}-g lightpaths can be routed via the set of all CMs, denoted by $\boldsymbol{M}$. Clearly, $\boldsymbol{M}_{K-1} = \boldsymbol{M}$.

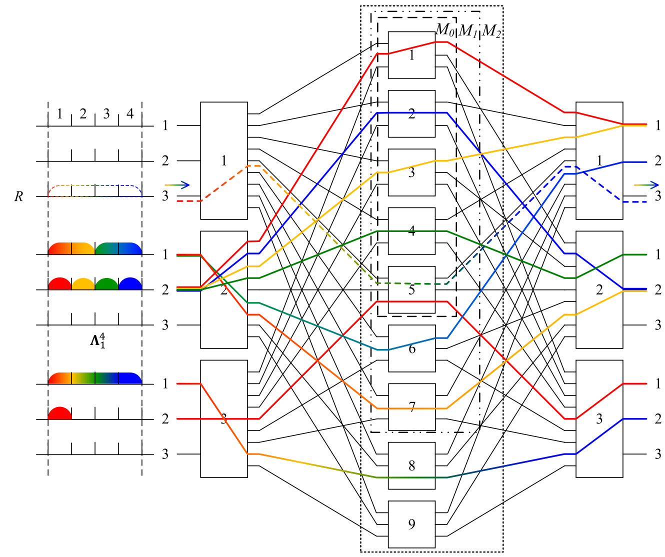

Fig. 7. Usage of the GDR strategy in $\mathcal{C}(3,3,9)$ under the GPuB model, where $\boldsymbol{M}_0 = \{1, 2, \cdots, 5\}$, $\boldsymbol{M}_1 = \{1, 2, \cdots, 7\}$, and $M_2 = \{1, 2, \cdots, 9\}$.

According to the GDR strategy, the OXC-Clos network finds an available CM in the set $\boldsymbol{M}_i$ by checking routing constraints C1 and C2. If several available CMs in $\boldsymbol{M}_i$ are found, the OXC-Clos network randomly selects one to route request R. Fig. 7 illustrates the GDR strategy and the routing process of a lightpath request. Assume that the OXC-Clos network needs to support 3 types of lightpaths, 1-g, 2-g, and 4-g lightpaths. According to the GDR strategy, the OXC-Clos network should assign the first 5 CMs for 1-g lightpaths, the first 7 CMs for 2-g lightpaths, and all the 9 CMs for 4-g lightpaths. Suppose that a 4-g request R arrives at IM 1 and heads to OM 1. The network will check all the 9 CMs to find one that is available for this request according to routing constraints C1 and C2. As we can see, CMs 2, 4, 5, 7, 8 and 9 are available for this request. The network then randomly selects one, say CM 5, from them for R. It is easy to know that the GDR strategy is quite simple and does not increase the operation complexity.

We will derive the minimal value of $|\boldsymbol{M}|$ and prove that $\mathcal{C}$ with the GDR strategy is WSNB when it needs to support K types of lightpaths. Before that, we need the following lemma.

Lemma 4: Consider J sets $\boldsymbol{F}_0, \boldsymbol{F}_1, \cdots, \boldsymbol{F}_{J-1}$ and $\widehat{\boldsymbol{F}}_j \triangleq \bigcup_{i=0}^{j} \boldsymbol{F}_i$, where $j = 0, 1, \cdots, J-1$. The following inequality
$$\sum_{j=0}^{J-1} \left(2^j \left|\boldsymbol{F}_j\right|\right) \geq 2^{J-1} \left|\widehat{\boldsymbol{F}}_{J-1}\right| - \sum_{j=0}^{J-2} \left(2^j \left|\widehat{\boldsymbol{F}}_j\right|\right)$$
always holds, and the inequality is satisfied with equality when $\boldsymbol{F}_0, \boldsymbol{F}_1, \cdots, \boldsymbol{F}_{J-1}$ are mutually disjoint.

Proof: Since
$$\left|\widehat{\boldsymbol{F}}_j\right| = \left|\widehat{\boldsymbol{F}}_{j-1}\right| + \left|\boldsymbol{F}_j\right| - \left|\widehat{\boldsymbol{F}}_{j-1} \cap \boldsymbol{F}_j\right|,$$
$\forall j = 1, 2, \cdots, J-1$, we have
$$\begin{aligned} &\sum_{j=0}^{J-1} \left(2^j \left|\boldsymbol{F}_j\right|\right) \\ &= \left|\boldsymbol{F}_0\right| + 2\left|\boldsymbol{F}_1\right| + \cdots + 2^j \left|\boldsymbol{F}_j\right| + \cdots + 2^{J-1}\left|\boldsymbol{F}_{J-1}\right| \\ &= \left|\widehat{\boldsymbol{F}}_0\right| + \cdots + 2^j \left(\left|\widehat{\boldsymbol{F}}_j\right| - \left|\widehat{\boldsymbol{F}}_{j-1}\right| + \left|\widehat{\boldsymbol{F}}_{j-1} \cap \boldsymbol{F}_j\right|\right) + \cdots \end{aligned}$$

$$\begin{aligned}&+2^{J-1}\left(\left|\widehat{\boldsymbol{F}}_{J-1}\right|-\left|\widehat{\boldsymbol{F}}_{J-2}\right|+\left|\widehat{\boldsymbol{F}}_{J-2}\cap \boldsymbol{F}_{J-1}\right|\right)\\ =&-\left|\widehat{\boldsymbol{F}}_{0}\right|-2\left|\widehat{\boldsymbol{F}}_{1}\right|-\cdots-2^{J-2}\left|\widehat{\boldsymbol{F}}_{J-2}\right|+2^{J-1}\left|\widehat{\boldsymbol{F}}_{J-1}\right|\\ &+\left(2\left|\widehat{\boldsymbol{F}}_{0}\cap \boldsymbol{F}_{1}\right|+\cdots+2^{J-1}\left|\widehat{\boldsymbol{F}}_{J-2}\cap \boldsymbol{F}_{J-1}\right|\right)\\ \geq&-\left|\widehat{\boldsymbol{F}}_{0}\right|-2\left|\widehat{\boldsymbol{F}}_{1}\right|-\cdots-2^{J-2}\left|\widehat{\boldsymbol{F}}_{J-2}\right|+2^{J-1}\left|\widehat{\boldsymbol{F}}_{J-1}\right|\\ =&2^{J-1}\left|\widehat{\boldsymbol{F}}_{J-1}\right|-\sum_{j=0}^{J-2}\left(2^{j}\left|\widehat{\boldsymbol{F}}_{j}\right|\right).\end{aligned}$$

It is clear that the equality holds when $\widehat{\boldsymbol{F}}_{j-1}\cap \boldsymbol{F}_{j}=\phi$, that is, $\boldsymbol{F}_0,\boldsymbol{F}_1,\cdots,\boldsymbol{F}_{J-1}$ are mutually disjoint. □

Under the GPB model, we only obtain the sufficient condition in general case for WSNB $\mathcal{C}$, which is required to support K types of lightpaths.

Theorem 2: $\mathcal{C}$ is WSNB for the 2^0-g, 2^1-g, $\cdots$, and 2^k-g lightpaths under the GPB model, if

$$m\geq 2n-1+k(n-1), \tag{6}$$

where $k=0,1,\cdots,K-1$.

Proof: Lemmas 1 and 3 show this theorem holds for $k=0$ and 1. We prove that if this theorem is true for $k=i$, where $i=2,3,\cdots,K-2$, it also holds for $k=i+1$.

Consider a 2^{i+1}-g request $R\left(\alpha,a,\beta,b,\boldsymbol{\Lambda}_w^{2^{i+1}}\right)$ that sees the following situation:

(a) p_α^j inputs of IM α and p_β^j outputs of OM β are busy in carrying 2^j-g lightpaths via $\boldsymbol{\Lambda}_w^{2^{i+1}}$, and
(b) $n-\sum_{j=0}^{i}p_\alpha^j-1$ inputs of IM α and $n-\sum_{j=0}^{i}p_\beta^j-1$ outputs of OM β are busy in carrying the last $K-i-1$ types of lightpaths via $\boldsymbol{\Lambda}_w^{2^{i+1}}$, and each port only carries one type of lightpaths,

where $p_\alpha^j,p_\beta^j=0,1,\cdots,n-1$ and $j=0,1,\cdots,i$. The total number of ports busy in $\boldsymbol{\Lambda}_w^{2^{i+1}}$ at IM α and OM β is $2n-2$.

Let $\boldsymbol{B}_j$ be the set of CMs used by the 2^j-g lightpaths that are carried by IM α or OM β via $\boldsymbol{\Lambda}_w^{2^{i+1}}$. Define

$$\widehat{\boldsymbol{B}}_j=\bigcup_{l=0}^{j}\boldsymbol{B}_l.$$

According to the GDR strategy and the induction hypothesis, all lightpaths in $\widehat{\boldsymbol{B}}_j$ can be routed via the CMs in $\boldsymbol{M}_j$ under the GDR strategy. Thus, there is

$$\left|\widehat{\boldsymbol{B}}_j\right|\leq\left|\boldsymbol{M}_j\right|. \tag{7}$$

Note that, for some combinations of n and i, the equality of (7) may be always unachievable in the GPB model. For example, consider the case where $i=2n-1$. As a port of $\mathcal{C}$ can only carry one type of lightpaths, R cannot see at least one type of lightpaths at the $2n-2$ ports busy in $\boldsymbol{\Lambda}_w^{2^{i+1}}$ at IM α and OM β. In this case, if the 2^j-g lightpath does not appear, there is

$$\left|\widehat{\boldsymbol{B}}_j\right|=\left|\widehat{\boldsymbol{B}}_{j-1}\right|\leq\left|\boldsymbol{M}_{j-1}\right|<\left|\boldsymbol{M}_j\right|,$$

where $j=1,2,\cdots,i$.

Let $\boldsymbol{S}_\alpha$ be the set of CMs used by the last $K-i-1$ types of lightpaths that occupy $\boldsymbol{\Lambda}_w^{2^{i+1}}$ and originate from IM α, and $\boldsymbol{S}_\beta$ be the set of CMs used by the last $K-i-1$ types of lightpaths that occupy $\boldsymbol{\Lambda}_w^{2^{i+1}}$ and visit OM β. Note that a lightpath with granularity larger than 2^i cannot employ the same CM with another one that also uses the FSUs in $\boldsymbol{\Lambda}_w^{2^{i+1}}$, if they share IM α or OM β. It follows that

$$\left|\boldsymbol{S}_\alpha\right|=n-\sum_{j=0}^{i}p_\alpha^j-1,$$

$$\left|\boldsymbol{S}_\beta\right|=n-\sum_{j=0}^{i}p_\beta^j-1,$$

and thus

$$\left|\boldsymbol{S}_\alpha\cup\boldsymbol{S}_\beta\right|\leq\left|\boldsymbol{S}_\alpha\right|+\left|\boldsymbol{S}_\beta\right|=2n-2-\sum_{j=0}^{i}\left(p_\alpha^j+p_\beta^j\right), \tag{8}$$

where the inequality holds with equality when $\boldsymbol{S}_\alpha\cap\boldsymbol{S}_\beta=\phi$.

$p_\alpha^j+p_\beta^j$ in (8) can be determined as follows. Any two 2^j-g lightpaths carried by p_α^j inputs of IM α or p_β^j outputs of OM β via $\boldsymbol{\Lambda}_w^{2^{i+1}}$ can share the same CM, as long as they do not use the same FSU. This implies that $|\boldsymbol{B}_j|$ must be less or equal to the number of these lightpaths. Also, the total number of FSUs in $\boldsymbol{\Lambda}_w^{2^{i+1}}$ on p_α^j inputs of IM α and p_β^j outputs of OM β is $2^{i+1}\left(p_\alpha^j+p_\beta^j\right)$, which can carry up to $2^{i-j+1}\left(p_\alpha^j+p_\beta^j\right)$ 2^j-g lightpaths according to A3. Thus, we have

$$\left|\boldsymbol{B}_j\right|\leq 2^{i-j+1}\left(p_\alpha^j+p_\beta^j\right).$$

Multiplying both sides of the inequality by 2^j and summing over all js, we have

$$\sum_{j=0}^{i}\left(2^j\left|\boldsymbol{B}_j\right|\right)\leq 2^{i+1}\sum_{j=0}^{i}\left(p_\alpha^j+p_\beta^j\right).$$

It follows that

$$\begin{aligned}\sum_{j=0}^{i}\left(p_\alpha^j+p_\beta^j\right)&\geq\left\lceil\frac{\sum_{j=0}^{i}\left(2^j\left|\boldsymbol{B}_j\right|\right)}{2^{i+1}}\right\rceil\\ &\geq\left\lceil\frac{2^i\left|\widehat{\boldsymbol{B}}_i\right|-\sum_{j=0}^{i-1}\left(2^j\left|\widehat{\boldsymbol{B}}_j\right|\right)}{2^{i+1}}\right\rceil\\ &\geq\left\lceil\frac{2^i\left|\widehat{\boldsymbol{B}}_i\right|-\sum_{j=0}^{i-1}\left(2^j\left|\boldsymbol{M}_j\right|\right)}{2^{i+1}}\right\rceil,\end{aligned} \tag{9}$$

where we use Lemma 4 for the second inequality, and (7) for the third inequality. It follows from (8) through (9) that the set of CMs that are not available for request R satisfies

$$\begin{aligned}&\left|\widehat{\boldsymbol{B}}_i\cup\boldsymbol{S}_\alpha\cup\boldsymbol{S}_\beta\right|\\ \leq&\left|\widehat{\boldsymbol{B}}_i\right|+\left|\boldsymbol{S}_\alpha\cup\boldsymbol{S}_\beta\right|\\ \leq&\left|\widehat{\boldsymbol{B}}_i\right|+2n-2-\sum_{j=0}^{i}\left(p_\alpha^j+p_\beta^j\right)\\ \leq&\left|\widehat{\boldsymbol{B}}_i\right|+2n-2-\left\lceil\frac{2^i\left|\widehat{\boldsymbol{B}}_i\right|-\sum_{j=0}^{i-1}\left(2^j\left|\boldsymbol{M}_j\right|\right)}{2^{i+1}}\right\rceil\\ \leq&\left|\boldsymbol{M}_i\right|+2n-2-\left\lceil\frac{2^i\left|\boldsymbol{M}_i\right|-\sum_{j=0}^{i-1}\left(2^j\left|\boldsymbol{M}_j\right|\right)}{2^{i+1}}\right\rceil\\ =&2n-1+i(n-1)+2n-2-n\\ =&2n-2+(i+1)(n-1),\end{aligned} \tag{10}$$

where we use Lemma 2 and (7) for the fourth inequality. Since we use (7) in the derivation of (10), the equality of (10) may be always unachievable for some combinations of n and i. It is thus only sufficient to show R can be satisfied if there are

$$m \geq 2n - 1 + (i+1)(n-1)$$

CMs, which proves this theorem. □

IV. WSNB Condition Under GPuB Model

Different from the GPB model, the GPuB model allows each port to carry various types of lightpaths simultaneously. It is obvious that the GPuB model provides more flexibility for bandwidth utilization of optical networks. In this section, we study the WSNB condition for OXC-Clos networks under the GPuB model, following the GDR strategy. Our results show that the flexibility comes with the slight increase of the cost of OXC-Clos networks.

Similar to Section III, this part proves the WSNB condition in an inductive manner. Following the GDR strategy and the arguments used in Section III, we have the following lemmas.

Lemma 5: $\mathcal{C}$ is SNB for 2^0-g lightpaths under the GPuB model iff $m \geq 2n-1$.

Lemma 6: $\mathcal{C}$ is WSNB for 2^0-g and 2^1-g lightpaths under the GPuB model iff $m \geq 3n-2$.

A. WSNB Condition

The GPuB model allows different types of lightpaths to share the same port. When $i \geq 2n-1$, a 2^{i+1}-g request from IM α to OM β could see all $i+2$ types of lightpaths in its required frequency slot at IM α and OM β under the GPuB model, which is different from the situation under the GPB model as we show in Theorem 2. Intuitively, the number of CMs occupied by the lightpaths that are carried by a given set of ports under the GPuB model would be larger than that under the GPB model. We will show that there always exists at least one case such that (7) holds with equality for any combination of n and i. Thus, the sufficient condition for WSNB OXC-Clos networks under the GPB model changes to the necessary and sufficient condition under the GPuB model, implying that the GPuB model increases the flexibility of bandwidth utilization only with a slightly increased cost.

Theorem 3: $\mathcal{C}$ is WSNB for the 2^0-g, 2^1-g, $\cdots$, and 2^k-g lightpaths under the GPuB model, iff

$$m \geq 2n - 1 + k(n-1), \tag{11}$$

where $k = 0, 1, \cdots, K-1$.

Proof: Lemmas 5 and 6 show this theorem holds for $k=0$ and 1. We prove that if this theorem is true for $k=i$, where $i = 2, 3, \cdots, K-2$, it also holds for $k=i+1$.

Consider a 2^{i+1}-g request $R\left(\alpha, a, \beta, b, \mathbf{\Lambda}_w^{2^{i+1}}\right)$, which sees the following situation:

(a) p_α inputs of IM α and p_β outputs of OM β are busy in carrying the first $i+1$ types of lightpaths via $\mathbf{\Lambda}_w^{2^{i+1}}$, and

(b) $n - p_\alpha - 1$ inputs of IM α and $n - p_\beta - 1$ outputs of OM β are busy in carrying the last $K-i-1$ types of lightpaths via $\mathbf{\Lambda}_w^{2^{i+1}}$,

where $p_\alpha, p_\beta = 0, 1, \cdots, n-1$.

Let $\boldsymbol{B}_j$ be the set of CMs used by the 2^j-g lightpaths that are carried by IM α or OM β via $\mathbf{\Lambda}_w^{2^{i+1}}$. Define $\widehat{\boldsymbol{B}}_j = \bigcup_{l=0}^{j} \boldsymbol{B}_l$. According to the GDR strategy and the induction hypothesis, all lightpaths in $\widehat{\boldsymbol{B}}_j$ can be routed via the CMs in $\boldsymbol{M}_j$ under the GDR strategy. Thus, there is

$$\left|\widehat{\boldsymbol{B}}_j\right| \leq \left|\boldsymbol{M}_j\right|. \tag{12}$$

Let $\boldsymbol{S}_\alpha$ be the set of CMs used by the last $K-i-1$ types of lightpaths that occupy $\mathbf{\Lambda}_w^{2^{i+1}}$ and originate from IM α, and $\boldsymbol{S}_\beta$ be the set of CMs used by the last $K-i-1$ types of lightpaths that occupy $\mathbf{\Lambda}_w^{2^{i+1}}$ and head for OM β. Note that a lightpath with granularity larger than 2^i cannot share the same CM with another one that also uses the FSUs in $\mathbf{\Lambda}_w^{2^{i+1}}$, if they share IM α or OM β. It follows that

$$|\boldsymbol{S}_\alpha| = n - p_\alpha - 1,$$
$$|\boldsymbol{S}_\beta| = n - p_\beta - 1,$$

and thus

$$|\boldsymbol{S}_\alpha \cup \boldsymbol{S}_\beta| \leq |\boldsymbol{S}_\alpha| + |\boldsymbol{S}_\beta| = 2\ nn - 2 - (p_\alpha + p_\beta), \tag{13}$$

where the inequality holds with equality when $\boldsymbol{S}_\alpha \cap \boldsymbol{S}_\beta = \phi$.

$p_\alpha + p_\beta$ in (13) can be determined as follows. Any two 2^j-g lightpaths carried by p_α inputs of IM α or p_β outputs of OM β via $\mathbf{\Lambda}_w^{2^{i+1}}$ can share the same CM, as long as they do not use the same FSU. This implies that the number of FSUs used by 2^j-g lightpaths should be larger than or equal to $2^j\left|\boldsymbol{B}_j\right|$. Also, the total number of FSUs in $\mathbf{\Lambda}_w^{2^{i+1}}$ on p_α inputs of IM α and p_β outputs of OM β is $2^{i+1}(p_\alpha + p_\beta)$. This implies

$$\sum_{j=0}^{i}\left(2^j\left|\boldsymbol{B}_j\right|\right) \leq 2^{i+1}(p_\alpha + p_\beta).$$

It follows that

$$\begin{aligned} p_\alpha + p_\beta &\geq \left\lceil \frac{\sum_{j=0}^{i}\left(2^j\left|\boldsymbol{B}_j\right|\right)}{2^{i+1}} \right\rceil \\ &\geq \left\lceil \frac{2^i\left|\widehat{\boldsymbol{B}}_i\right| - \sum_{j=0}^{i-1}\left(2^j\left|\widehat{\boldsymbol{B}}_j\right|\right)}{2^{i+1}} \right\rceil \\ &\geq \left\lceil \frac{2^i\left|\widehat{\boldsymbol{B}}_i\right| - \sum_{j=0}^{i-1}\left(2^j\left|\boldsymbol{M}_j\right|\right)}{2^{i+1}} \right\rceil. \end{aligned} \tag{14}$$

where we use Lemma 4 for the second inequality, and (12) for the third inequality. It follows from (13) through (14) that the set of CMs that are not available for request R satisfies

$$\begin{aligned} &\left|\widehat{\boldsymbol{B}}_i \cup \boldsymbol{S}_\alpha \cup \boldsymbol{S}_\beta\right| \\ \leq &\left|\widehat{\boldsymbol{B}}_i\right| + |\boldsymbol{S}_\alpha \cup \boldsymbol{S}_\beta| \\ \leq &\left|\widehat{\boldsymbol{B}}_i\right| + 2n - 2 - (p_\alpha + p_\beta) \\ \leq &\left|\widehat{\boldsymbol{B}}_i\right| + 2n - 2 - \left\lceil \frac{2^i\left|\widehat{\boldsymbol{B}}_i\right| - \sum_{j=0}^{i-1}\left(2^j\left|\boldsymbol{M}_j\right|\right)}{2^{i+1}} \right\rceil \\ \leq &\left|\boldsymbol{M}_i\right| + 2n - 2 - \left\lceil \frac{2^i\left|\boldsymbol{M}_i\right| - \sum_{j=0}^{i-1}\left(2^j\left|\boldsymbol{M}_j\right|\right)}{2^{i+1}} \right\rceil \\ = &2n - 1 + i(n-1) + 2n - 2 - n \\ = &2n - 2 + (i+1)(n-1). \end{aligned} \tag{15}$$

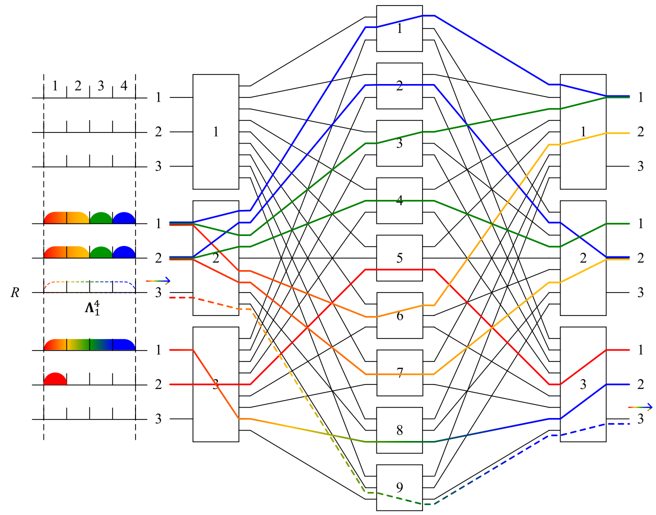

Fig. 8. $R\left(2,3,3,3,\mathbf{\Lambda}_1^4\right)$ sees the worst case in $\mathcal{C}\left(3,3,9\right)$ under the GPuB model.

where the fourth inequality follows from Lemma 2 and (12). For arbitrary $n \geq 2$ and i, the inequality of (15) is satisfied with equality, if request R sees the following situation when it arrives:

(i) In IM α, each of $n-1$ inputs carries 2 2^0-g lightpaths and i lightpaths, the granularities of which are $2^1, 2^2, \cdots, 2^i$. All the lightpaths are allocated in $\mathbf{\Lambda}_w^{2^{i+1}}$ side-by-side in decreasing order of the granularity, so that each of them is carried by a frequency slot defined by assumption A3. IM α carries $2(n-1)$ 2^0-g lightpaths and $n-1$ 2^j-g lightpaths in total, where $j = 1, 2, \cdots, i$.

(ii) In OM β, one output carries a 2^0-g lightpath via $\mathbf{\Lambda}_w^{2^{i+1}}$, and each of other $n-2$ outputs carries a 2^{i+1}-g lightpath via $\mathbf{\Lambda}_w^{2^{i+1}}$. OM β carries 1 2^0-g lightpath and $n-2$ 2^{i+1}-g lightpaths in total.

All the lightpaths in (i) and (ii) are different and use different CMs, and $2n-1$ 2^0-g lightpaths are routed via the CMs in

$$\boldsymbol{B}_0 = \left\{1, 2, \cdots, 2n-1\right\},$$

and $n-1$ 2^j-g lightpaths are routed via the CMs in

$$\boldsymbol{B}_j = \left\{2n+(j-1)(n-1), \cdots, 2n-1+j(n-1)\right\},$$

where $j = 1, \cdots, i$, and $n-2$ 2^{i+1}-g lightpaths are routed via the CMs in

$$\boldsymbol{B}_{i+1} = \left\{2n+i(n-1), \cdots, 2n-2+(i+1)(n-1)\right\},$$

which is consistent with the GDR strategy. It thus needs $m \geq 2n-1+(i+1)(n-1)$ CMs to satisfy R. □

Fig. 8 plots a $\mathcal{C}\left(3,3,9\right)$ where 3 types of lightpaths coexist. According to the GDR strategy, $|\boldsymbol{M}_0| = 5$ and $|\boldsymbol{M}_1| = 7$. A request $R\left(2,3,3,3,\mathbf{\Lambda}_1^4\right)$ sees the following situation:

(i) In IM 2, inputs 1 and 2 each carry a 2-g lightpath via $\mathbf{\Lambda}_1^2$ including FSUs 1 and 2, and 2 1-g lightpaths via $\mathbf{\Lambda}_3^1$ including FSU 3 and $\mathbf{\Lambda}_4^1$ including FSU 4. IM 2 carries 2 2-g lightpaths and 4 1-g lightpahts in total.

(ii) In OM 3, output 1 carries a 1-g lightpath using $\mathbf{\Lambda}_1^1$, and output 2 carries a 4-g lightpath using $\mathbf{\Lambda}_1^4$.

Specifically, 5 1-g lightpaths are routed via CMs 1 through 5, 2 2-g lightpaths via CMs 6 and 7, and 1 4-g lightpath via CM 8, which is consistent with the GDR strategy. We thus need one more CM (i.e., 9 CMs in total) to satisfy R.

B. Discussion

The WSNB flex-grid OXC-Clos network investigated in this paper is superior to an SNB network in system cost. This can be found by comparing (6), (11) and (1). With the assistance of the GDR strategy, the number of the CMs needed by a WSNB network is $2n-1+K(n-1)$, which is much smaller than that of the CMs needed by an SNB network, i.e., $2^K(n-1)+1$.

Also, the WSNB network under study almost maintains the same nonblocking property as an SNB network. Similar to an SNB network, the WSNB network can set up a new lightpath without any reconfiguration. The sole difference lies in that it requires assistance from the GDR strategy, which merely specifies the sets of the CMs that can be employed by different types of lightpaths and, consequently, does not introduce any routing complexity. That is, the WSNB network, leveraging the GDR strategy, preserves the identical nonblocking property as an SNB network, while incurring no additional operational complexity costs.

When $K = 1$, the flex-grid OXC-Clos network changes to a fixed-grid switching network. In this case, (6) and (11) change to $m \geq 2n-1$, indicating that the SNB and WSNB OXC-Clos networks have the same cost, which is consistent with the result of [20]. This also verifies the correctness of our results.

V. Effect of GDR Strategy Under Other Granularity Patterns

This section demonstrates that the GDR strategy can also reduce the number of required CMs under other granularity patterns. Specifically, we consider a linear granularity pattern, where the granularity of lightpaths increases according to natural numbers. We demonstrate the effectiveness of the GDR strategy by enumeration, since we do not have the closed-form WSNB condition of flex-grid OXC-Clos networks with linear granularity pattern by now.

A. Linear Granularity Pattern and SNB Condition

Assume that there are K types of frequency slots in the optical network. The linear granularity pattern can be formally defined as follows.

L1. There are W FSUs, where W is the common multiple of $1, 2, \cdots, K$,

L2. The k-th type of lightpath occupies k adjacent FSUs, where $k = 1, 2, \cdots, K$, and the set of FSUs of the i-th k-g frequency slot is defined by the set

$$\mathbf{\Lambda}_{k(i-1)+1}^k = \left\{k(i-1)+1, \cdots, ki\right\},$$

where $i = 1, 2, \cdots, W/k$.

Using the similar argument in Section II, the SNB condition under the linear granularity pattern can be easily obtained.

Theorem 4: When K types of lightpaths coexist, $\mathcal{C}(n,r,m)$ is SNB iff

$$m \geq 2K(n-1)+1.$$

B. Effectiveness of GDR Strategy

The WSNB condition under the linear granularity pattern is different from that under the exponential granularity pattern. In this pattern, the number of FSUs in a large-granularity frequency slot is not the integer multiple of the number of FSUs

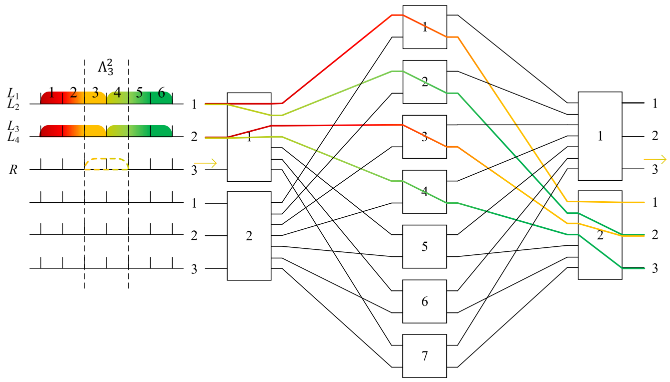

Fig. 9. Example of an OXC-Clos network with linear granularity pattern.

in the small-granularity one. Thus, the FSU occupation seen by a request under the linear pattern is quite different from that under the exponential pattern. For example, consider a k-g request $R(\alpha, a, \beta, b, \mathbf{\Lambda}^k_{k(i-1)+1})$, where $i = 1, 2, \cdots, W/k$. The frequency slot $\mathbf{\Lambda}^k_{k(i-1)+1}$ on other $n-1$ inputs of IM α could be occupied by $2(n-1)$ lightpaths with the granularity larger than k. Fig. 9 illustrates a 2-g request $R(1, 3, 1, 3, \mathbf{\Lambda}^2_3)$, and the frequency slot $\mathbf{\Lambda}^2_3$ at IM 1 are used by 4 3-g lightpaths. This situation will never occur under the exponential granularity pattern, which in turn makes the derivation of the closed-form WSNB condition under the linear granularity pattern difficult.

We study the WSNB condition case by case under different values of n and K. For each pair of n and K, we follow the GDR strategy and seek the worst case by enumerating all possible CM occupations. Fig. 10 compares the SNB condition with the WSNB condition when $n \leq 7$ and $K \leq 6$. Simulation results clearly demonstrate that the GDR strategy can reduce the number of CMs required to perform nonblocking switching functions under both the GPB model and the GPuB model. Once again, we find that the number of CMs needed by WSNB networks under the GPuB model is slightly larger than that under the GPB model, which is similar to the result presented in Sections III and IV. This verifies that our enumeration is correct.

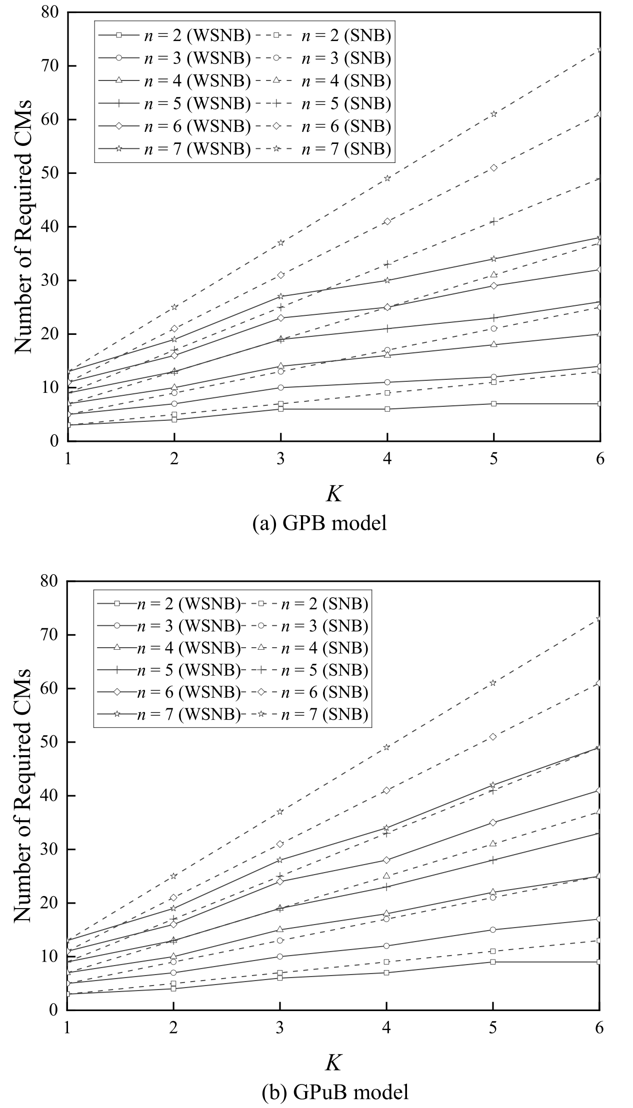

Fig. 10. Comparison of the SNB and WSNB conditions under the linear granularity pattern.

VI. Application to Multifiber Networks

In this section, we discuss the application of WSNB OXC-Clos network to the multi-fiber flex-grid networks.

A. Node Design

Consider a ROADM with a nodal degree, denoted as Δ, which is defined as the number of ROADMs that it connects with in the optical network. Though the number of fibers on different degrees could be different in practice, we consider the case where all the degrees have the same number of fibers, denoted by F, to facilitate the presentation. This ROADM has ΔF input directions and ΔF output directions. Additionally, the ROADM needs some add ports to add local wavelengths to output directions, and some drop ports to drop remote wavelengths. Let r_{ad} be the add/drop ratio, which is the ratio of the number of add/drop ports to that of input/output directions. The number of add/drop ports can then be calculated as $\Delta F r_{ad}$.

Such a ROADM needs an $N \times N$ OXC-Clos network, where $N = \Delta F(1 + r_{ad})$. A typical nodal degree Δ ranges from 2 to 8, and $0 < r_{ad} \leq 1$. Consider the case where N and F are large, and suppose the number of inputs/outputs of IMs/OMs n can divide F evenly. By treating each port of the OXC-Clos network as one direction of the ROADM, every F/n IMs (F/n OMs) are grouped together to serve an input (output) degree, respectively. In total, the inputs of $\Delta F/n$ IMs and the outputs of $\Delta F/n$ OMs are used to connect with other Δ ROADMs in the network. Similarly, $\Delta F r_{ad}/n$ IMs and $\Delta F r_{ad}/n$ OMs serve for the purposes of wavelength adding and dropping, respectively. Fig. 11 plots an example, where $\Delta = 4$, $F = 8$, $r_{ad} = 25\%$, and $n = 4$. Suppose that the network carries $K = 3$ types of lightpaths and the granularity pattern is exponential. To fulfill a WSNB switching function, the OXC-Clos network needs $m = 13$ CMs, according to Theorem 2 or 3. As Fig. 11 plots, IMs 1 through 8 and OMs 1 through 8 connect with other ROADM nodes, and IMs 9 and 10 and OMs 9 and 10 link to the local wavelength add/drop systems.

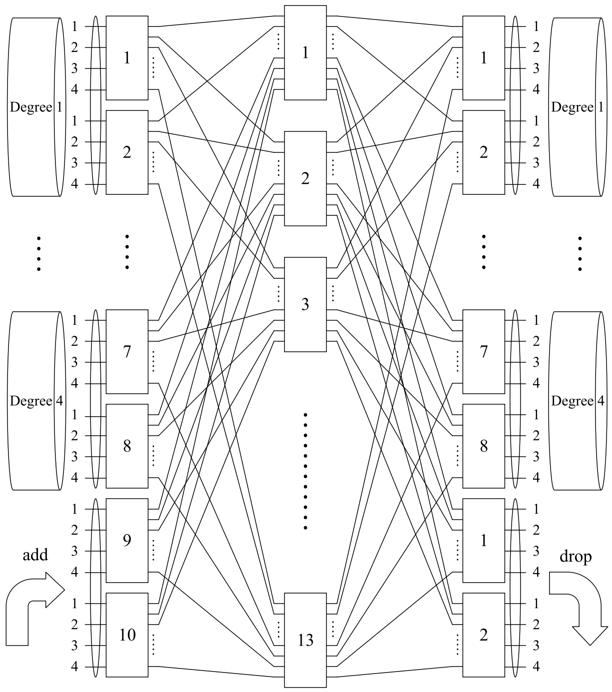

Fig. 11. Implementation of a WSNB OXC in a ROADM system supporting multiple fibers per degree.

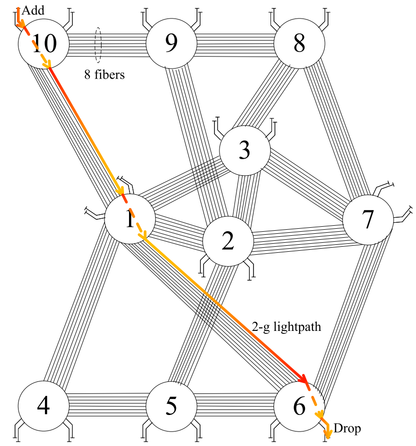

Fig. 12. Illustration of the establishment of a 2-g network-level lightpath.

In an optical node, there is no lightpath established from the add ports to the drop ports. For example, IM 9 or IM 10 will never generate a request to visit OM 9 or IM 10 in Fig. 11.

We also consider the physical performance and the cost of ROADMs when applying the OXC-Clos network. A classical OXC has an insertion loss of around 15 dB. We need an ingress EDFA and an egress EDFA at each input and each output to compensate the loss, when the classical OXC is deployed. For the OXC-Clos network, we have to install two columns of EDFAs before and after the CMs, in addition to the ingress and egress EDFAs. Thus, a lightpath from an input to an output has to pass through 4 EDFAs in the OXC-Clos network, as compared with the 2 EDFAs in the classical OXC. Based on the study in [21], the classical OXC can support as many as 30 cascaded OXCs with less than 1 dB penalty. This implies the OXC-Clos network can support at least 15 cascaded OXCs, which can cover about 99% application scenarios in practical networks [22]. On the other hand, the WSSs will introduce filtering effect. Previous studies show that the filtering due to cascaded WSSs does not have much impact on optical signal performance for the mainstream modulation formats [23], [24]. The above discussions indicate that OXC-Clos network is acceptable in transmission performance degradation. At last, under the case where $r = n = \sqrt{N}$, an $N \times N$ WSNB OXC-Clos network requires $(4 + 2K)N - 2(K + 1)\sqrt{N}$ more EDFAs than an $N \times N$ classical OXC. This number is reasonable given that the dimension of OXC is very high.

B. Network Application

From a network-wide perspective, the network-level routing (i.e., the routing in a whole optical network) and the node-level routing have no dependence, provided each switching node is nonblocking. To avoid confusion, we define a lightpath from a source to a destination in an optical network as network-level lightpath, whereas define a lightpath from an input to an output of an OXC node as node-level lightpath. When a network-level lightpath request arrives, the optical network assigns to it a path from the source to the destination and a frequency slot on the links along this path, using RSA algorithms, such as the algorithms reported in [3] and [7]. The allocation then triggers a node-level lightpath request in each node on the path. Fig. 12 illustrates an example, where each link installs 8 fibers. The network assigns a path and a 2-g frequency slot on the links along this path for a 2-g network-level lightpath request from node 10 to node 6. Suppose that the first fiber of each link is assigned to the network-level lightpath. After that, each node on the path has to create a 2-g node-level lightpath to complete the establishment of the network-level lightpath. For example, node 1 needs to establish a 2-g node-level lightpath from fiber 1 of its input link connected with node 10 to fiber 1 of its output link connected with node 6. In this case, node 1 uses the GDR strategy to find a proper CM to establish a node-level lightpath. The WSNB property of each node ensures that the node-level lightpath can always be set up successfully. That is, if the optical node is nonblocking, a network-level lightpath from the source to the destination can be set up as long as the source has free transmitters, the destination has idle receivers, and an available frequency slot can be found along a path from the source to the destination.

In contrast, the situation is different if the node is blocking. In this case, joint network-level and node-level routing would be a key to lower the blocking probability of lightpath requests. Otherwise, the blocking probability could be high. The reason is self-evident. Consider the case in Fig. 12, and imagine that the node is blocking. In this case, though the RSA algorithm can identify a path and a 2-g frequency slot along that path, the network-level lightpath request can still be blocked if any one of the nodes along that path fails to establish a node-level lightpath. This is precisely why the RSA algorithm developed by Ref. [25] also considers the internal state of nodes.

The above discussion clearly shows that the network-level routing and the node-level routing can be decoupled, and thus the RSA process can be simplified if the OXC nodes are all nonblocking, as we have mentioned in Section I. The blocking performance of the optical network in this case is completely determined by the RSA algorithm.

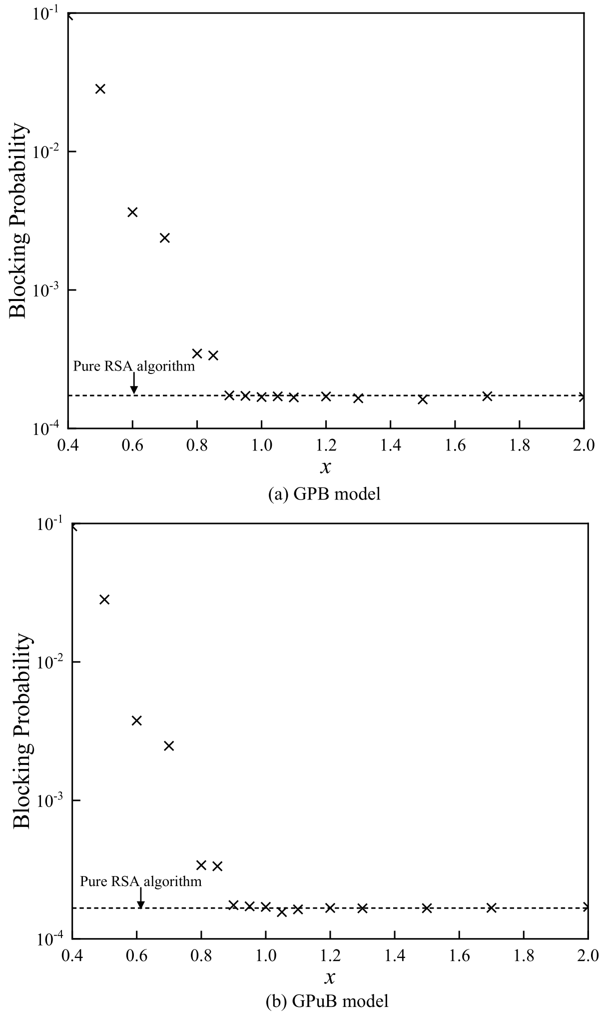

Fig. 13. Blocking probabilities of network-level lightpaths in CERNET under (a) the GPB model and (b) the GPuB.

Herein, we verify this point via simulation. Define x as the ratio of the number of CMs in each node to that required by the WSNB condition. All the nodes are WSNB if $x \geq 1$, and are blocking if $x < 1$. We demonstrate that the blocking probability of a network equipped with the OXC nodes with $x \geq 1$ is completely determined by the RSA algorithm. In the simulation, we use a simple RSA algorithm to set up an end-to-end lightpath for a network-level request. Specifically, we find a shortest path using Dijkstra's algorithm, and search for a frequency slot commonly available on the links on that path using the first-fit approach. We then assign the available fiber with the lowest index to the network-level request. At last, we apply the GDR strategy to build a node-level lightpath in each node on the path. A network-level request is blocked if the RSA algorithm fails to find a path or a frequency slot along that path, or if any one of the nodes on the path fails to build up a node-level lightpath after the RSA is completed. We take the CERNET [26] in Fig. 12 as an example, where the number of fibers on each link is 8. The network needs to support 3 types of lightpaths, i.e., 1-g, 2-g, and 4-g lightpaths. We simulate 10^7 network-level requests, where three types of requests are generated with equal probability. The simulation results in Fig. 13 clearly show that the blocking probability of network-level lightpath requests decreases as x increases, and converges to that of the RSA algorithm when x approaches 1.

VII. Related Works

Several designs [27], [28], [29], [30], [31], [32], [33], [34], [35], [36], [37], [38] have been proposed to improve the scalability of OXCs at the expense of nonblocking property. A multi-stage heterogeneous OXC was devised in [27], the idea of which is to decompose each $1 \times N$ WSS in the standard OXC to a two-stage WSS structure and replace each WSS in the second stage by a wavelength-insensitive optical space switch. Another type of large-scale OXC is the interconnection of several OXCs in a ring topology [33], [34], [35], [36]. Both of them are internally blocking. Applying such an internally-blocking OXC to the optical network will remarkably complicate the process of routing and spectrum allocation [13], [25].

The earliest Clos network that is able to support connections of different granularities at the same time is the multi-rate Clos network [12], [15], [16], [17], [18] studied in the 1990s. The multi-rate Clos network is quite different from the flex-grid OXC-Clos network. First, the former is an electrical switching network. Second, a nonblocking multi-rate Clos network can establish a connection from an input to an output, as long as the input and the output can provide enough bandwidth to accommodate the request. The bandwidth at the input and the output could be composed of several different or discontinuous spectrum segments. In contract, a nonblocking flex-grid switching network can set up a lightpath, only when the input and the output have a common continuous optical spectrum that can accommodate the request. Thus, the nonblocking conditions of multi-rate Clos networks [12], [15], [16], [17], [18] cannot be directly applied to flex-grid OXC-Clos networks.

Two kinds of Clos-like flex-grid optical switches, called space-wavelength-space (SWS) switch and wavelength-space-wavelength (WSW) switch, were proposed in [39], [40], and [41]. In the SWS switch, each IM and each OM are OXCs, and each CM is a bandwidth-variable wavelength-converting switch (BV-WS), which is an OXC embedded with bandwidth-variable tunable waveband converters (BV-TWBCs). In the WSW switch, each IM and each OM are BV-WSs, while each CM is an OXC. References [39] and [41] derived the SNB conditions, which specify the number of CMs needed for the SWS switch and the WSW switch to achieve SNB property. However, it is known that all-optical tunable WC and BV-TWBC are not commercially available. At the current stage, it would be valuable to investigate the flex-grid Clos network without WCs.

References [42], [43], and [44] reported the WSNB conditions for the WSW switches based on the idea of the functional decomposition of central switch modules. This strategy divides the connections into several classes according to their bandwidth requirements, and partitions the central switch modules into several disjoint sets. Each set of middle-stage switches only serves one class of connections. While the strategies in [42], [43], and [44] follow a decomposition approach, our GDR strategy adopts an inclusive approach in assigning the CMs, where the CM set assigned to small-granularity

TABLE I
COMPARISON OF SEVERAL SCALABLE OXCS

	nonblocking	flex-grid	WC needed?
HIER [27]	no	no	no
Ring-type OXC [33]–[36]	no	yes	no
HOXC [37], [38]	no	yes	no
WSW [40]	yes	yes	yes
SWS [39], [41]	yes	yes	yes
OXC-Clos network [45]–[47]	yes	no	no
WSNB OXC-Clos network	yes	yes	no

WC: wavelength converter

lightpaths is a subset of that allocated to large-granularity lightpaths. Consider an OXC-Clos network that has to carry K types of lightpaths, with the granularity of each type increasing exponentially. It is easy to show that the number of CMs needed by such an OXC-Clos network using the strategy in [42], [43], and [44] is not smaller than $K(2n-1)$, which is clearly larger than the number of CMs needed by an OXC-Clos network using the GDR strategy as long as $K > 1$.

References [45], [46], and [47] constructed large-scale OXCs based on Clos network. Specially, [45] studied the ability of OXC-Clos network with and without WCs to establish a lightpath from an input to an output if there are idle transmitters at the input and idle receivers at the output, and obtained the SNB conditions, which specify the numbers of CMs and wavelengths needed to fulfill SNB switching function. These three papers did not explore the nonblocking conditions in the flex-grid scenario.

In summary, Table I presents the comparison of the WSNB OXC-Clos network studied in this paper with the scalable OXC structures proposed in recent years.

VIII. CONCLUSION

This paper studies the nonblocking conditions for the flex-grid OXC-Clos network without wavelength converters. The main contribution is to propose the GDR strategy and seek the WSNB conditions. The idea of the GDR is to restrict the usage of CMs by the lightpaths of different granularities, thereby leaving more CMs for large-granularity requests. Under this strategy, we prove the WSNB conditions and show that the cost of WSNB OXC-Clos network is remarkably smaller than that of SNB OXC-Clos network. We study two system models, the GPB model and GPuB model. We demonstrate that, compared to the GPB model, the GPuB model leads to more flexibility in network-bandwidth utilization only at a small cost of switching fabrics.

REFERENCES

[1] P. J. Winzer, D. T. Neilson, and A. R. Chraplyvy, "Fiber-optic transmission and networking: The previous 20 and the next 20 years," *Opt. Exp.*, vol. 26, no. 18, pp. 24190–24239, 2018.

[2] O. Gerstel, M. Jinno, A. Lord, and S. J. B. Yoo, "Elastic optical networking: A new dawn for the optical layer?" *IEEE Commun. Mag.*, vol. 50, no. 2, pp. s12–s20, Feb. 2012.

[3] Y. Yin, M. Zhang, Z. Zhu, and S. J. B. Yoo, "Fragmentation-aware routing, modulation and spectrum assignment algorithms in elastic optical networks," in *Proc. IEEE OFC*, Mar. 2013, pp. 1–3.

[4] V. López et al., "Elastic optical networks," *Architectures, Technologies, and Control*. Cham, Switzerland: Springer, 2016.

[5] B. Chatterjee and E. Oki, *Elastic Optical Networks: Fundamentals, Design, Control, and Management*. Boca Raton, FL, USA: CRC Press, 2020.

[6] Ì. Brasileiro, L. Costa, and A. Drummond, "A survey on challenges of spatial division multiplexing enabled elastic optical networks," *Opt. Switching Netw.*, vol. 38, Sep. 2020, Art. no. 100584.

[7] Y. Qiu, "Group-based spectrum assignment in dynamic flex-grid optical networks," *Opt. Fiber Technol.*, vol. 19, no. 5, pp. 437–445, Oct. 2013.

[8] FINISAR. (Oct. 2021). *Flexgrid Twin 1x48 Wavelength Selective Switch*. [Online]. Available: https://www.globenewswire.com/news-release/2021/10/04/2307857/0/en/Finisar-Australia-Releases-the-World-s-First-Flexgrid-Twin-1x48-Wavelength-Selective-Switch.html

[9] C. Clos, "A study of non-blocking switching networks," *Bell Syst. Tech. J.*, vol. 32, no. 2, pp. 406–424, Mar. 1953.

[10] V. E. Beneš, *Mathematical Theory of Connecting Networks and Telephone Traffic*. New York, NY, USA: Academic, 1965.

[11] S. C. Liew and T. T. Lee, *Principles of Broadband Switching and Networking*. Hoboken, NJ, USA: Wiley, 2010.

[12] S. C. Liew, M.-H. Ng, and C. W. Chan, "Blocking and nonblocking multirate clos switching networks," *IEEE/ACM Trans. Netw.*, vol. 6, no. 3, pp. 307–318, Jun. 1998.

[13] M. Ge, T. Ye, T. T. Lee, and W. Hu, "Multicast routing and wavelength assignment in AWG-based clos networks," *IEEE/ACM Trans. Netw.*, vol. 25, no. 3, pp. 1892–1909, Jun. 2017.

[14] T. Ye, T. T. Lee, and W. Hu, "AWG-based non-blocking clos networks," *IEEE/ACM Trans. Netw.*, vol. 23, no. 2, pp. 491–504, Apr. 2015.

[15] R. Melen and J. S. Turner, "Nonblocking multirate networks," *SIAM J. Comput.*, vol. 18, no. 2, pp. 301–313, Apr. 1989.

[16] E. Valdimarsson, "Blocking in multirate interconnection networks," *IEEE Trans. Commun.*, vol. 42, nos. 2–4, pp. 2028–2035, Feb. 1994.

[17] J. S. Turner and R. Melen, "Multirate clos networks," *IEEE Commun. Mag.*, vol. 41, no. 10, pp. 38–44, Oct. 2003.

[18] B. Gao and F. K. Hwang, "Wide-sense nonblocking for multirate 3-stage clos networks," *Theor. Comput. Sci.*, vol. 182, nos. 1–2, pp. 171–182, Aug. 1997.

[19] *Spectral Grids for WDM Applications: DWDM Frequency Grid*, document ITU-T Std. G.694.1, 2012.

[20] K.-H. Tsai, D.-W. Wang, and F. Hwang, "Lower bounds for wide-sense nonblocking clos network," *Theor. Comput. Sci.*, vol. 261, no. 2, pp. 323–328, Jun. 2001.

[21] D. G. Sequeira, L. G. Cancela, and J. L. Rebola, "Impact of physical layer impairments on multi-degree CDC ROADM-based optical networks," in *Proc. IEEE ONDM*, May 2018, pp. 94–99.

[22] FINISAR. (Apr. 2023). *Too Many ROADMs? ICE6 Can Help*. [Online]. Available: https://www.infinera.com/blog/too-many-roadms-ice6-can-help/tag/optical/

[23] N. Deng et al., "Performance challenges and key technologies of all-optical cross-connect network filtering effect," *Huawei Res. J.*, vol. 4, pp. 98–108, Jan. 2023.

[24] J. C. Cartledge, "Performance of coherent optical fiber transmission systems," *Frontiers Optoelectronics*, vol. 11, no. 2, pp. 128–133, Jun. 2018.

[25] K. Sato, Y. Mori, H. Hasegawa, and K.-I. Sato, "Algorithm for raising OXC port count to meet traffic growth at minimum cost," *J. Opt. Commun. Netw.*, vol. 9, no. 2, pp. A263–A270, Feb. 2017.

[26] Y. Liu, "Current situation and prospect of CERNET," in *China's E-Science Blue Book 2020*. Singapore: Springer, 2021, pp. 327–334.

[27] T. Ban, H. Hasegawa, K.-I. Sato, T. Watanabe, and H. Takahashi, "A novel large-scale OXC architecture that employs wavelength path switching and fiber selection," in *Proc. IEEE ECOC*, Sep. 2012, pp. 1–3.

[28] H. Minami et al., "Experimental demonstration of cascadable PPLN-based inter-band wavelength converters for band-switchable multi-band optical cross-connect," in *Proc. IEEE OFC*, Mar. 2023, pp. 1–3.

[29] T. Kuno, Y. Mori, S. Subramaniam, M. Jinno, and H. Hasegawa, "Experimental evaluation of optical cross-connects with flexible waveband routing function for SDM networks," in *Proc. IEEE OFC*, Jun. 2021, pp. 1–3.

[30] T. Ishikawa, Y. Mori, H. Hasegawa, S. Subramaniam, K.-I. Sato, and O. Moriwaki, "Compact OXC architecture, design and prototype development for flexible waveband routing optical networks," *Opt. Exp.*, vol. 25, no. 14, p. 15838, 2017.

[31] T. Kodama, T. Ishikawa, D. Suzuki, and M. Jinno, "Demonstration of any-care-access non-directional spatial cross-connects based on core selective switch with and without core-contention constraint," in *Proc. IEEE ECOC*, Dec. 2020, pp. 1–4.

[32] H. Kawahara, M. Nakagawa, T. Seki, and T. Miyamura, "Experimental demonstration of wavelength-selective Band/Direction-switchable multi-band OXC using an inter-band all-optical wavelength converter," in *Proc. IEEE ECOC*, Dec. 2020, pp. 1–4.

[33] Y. Iwai, H. Hasegawa, and K.-i. Sato, "OXC hardware scale reduction attained by using interconnected subsystem architecture," in *Proc. IEEE OFC*, Mar. 2013, pp. 1–3.

[34] H. Ishida, H. Hasegawa, and K.-I. Sato, "Hardware scale and performance evaluation of a compact subsystem modular optical cross connect that adopts tailored add/drop architecture," *J. Opt. Commun. Netw.*, vol. 7, no. 6, pp. 586–595, Jun. 2015.

[35] H. Hasegawa and K.-I. Sato, "Large scale optical cross-connect: Architecture, performance analysis, and feasibility demonstration," in *Proc. IEEE OFC*, Mar. 2015, pp. 1–3.

[36] Y. Iwai, H. Hasegawa, and K.-I. Sato, "Large-scale photonic node architecture that utilizes interconnected small scale optical cross-connect sub-systems," in *Proc. IEEE ECOC*, Sep. 2012, pp. 1–3.

[37] M. Jinno, "Spatial channel cross-connect architectures for spatial channel networks," *IEEE J. Sel. Topics Quantum Electron.*, vol. 26, no. 4, pp. 1–16, Jul. 2020.

[38] K. Nakada et al., "Single multicore-fiber bidirectional spatial channel network based on spatial cross-connect and multicore EDFA efficiently accommodating asymmetric traffic," in *Proc. IEEE OFC*, Mar. 2023, pp. 1–3.

[39] W. Kabacinski, M. Michalski, and R. Rajewski, "Strict-sense nonblocking W-S-W node architectures for elastic optical networks," *J. Lightw. Technol.*, vol. 34, no. 13, pp. 3155–3162, Apr. 28, 2016.

[40] G. Danilewicz, W. Kabacinski, and R. Rajewski, "Strict-sense nonblocking space- wavelength-space switching fabrics for elastic optical network nodes," *J. Opt. Commun. Netw.*, vol. 8, no. 10, pp. 745–756, Oct. 2016.

[41] W. Kabacinski, M. Michalski, and M. Abdulsahib, "The strict-sense nonblocking elastic optical switch," in *Proc. IEEE HPSR*, Jul. 2015, pp. 1–6.

[42] W. Kabacinski and M. Abdulsahib, "Wide-sense nonblocking converting-space-converting switching node architecture under XsVarSWITCH control algorithm," *IEEE/ACM Trans. Netw.*, vol. 28, no. 4, pp. 1550–1561, Aug. 2020.

[43] W. Kabaciński, M. Michalski, and M. Abdulsahib, "Wide-sense nonblocking elastic optical switch," *Opt. Switching Netw.*, vol. 25, pp. 71–79, Jul. 2017.

[44] G. Danilewicz, "Asymmetrical space-conversion-space SCS1 strict-sense and wide-sense nonblocking switching fabrics for continuous multislot connections," *IEEE Access*, vol. 7, pp. 107058–107072, 2019.

[45] J. Lin, T. Chang, Z. Zhai, S. K. Bose, and G. Shen, "Wavelength selective switch-based clos network: Blocking theory and performance analyses," *J. Lightw. Technol.*, vol. 40, no. 17, pp. 5842–5853, Jun. 27, 2022.

[46] K. Chen, T. Ye, H. He, and Z. Guo, "Modular optical cross-connects (OXCs) for large-scale optical networks," *IEEE Photon. Technol. Lett.*, vol. 31, no. 10, pp. 763–766, Mar. 22, 2019.

[47] H. Mehrvar, S. Li, and E. Bernier, "Dimensioning networks of ROADM cluster nodes," *J. Opt. Commun. Netw.*, vol. 15, no. 8, pp. C166–C178, Aug. 2023.

Yibei Yao received the B.S. degree in communication engineering from Tongji University, Shanghai, China, in 2022. She is currently pursuing the M.S. degree with the Department of Electronic Engineering, Shanghai Jiao Tong University, Shanghai.

Her research interests include optical cross-connect and optical networks.

Tong Ye (Member, IEEE) received the B.S. and M.S. degrees from the University of Electronic Science and Technology of China, Chengdu, China, in 1998 and 2001, respectively, and the Ph.D. degree in electronics engineering from Shanghai Jiao Tong University, Shanghai, China, in 2005.

He was with The Chinese University of Hong Kong, Hong Kong, for one and a half years as a Post-Doctoral Research Fellow. He is currently an Associate Professor with the State Key Laboratory of Photonics and Communications, Shanghai Jiao Tong University. His research interests include optical interconnection and switching networks, optical datacenter networks, and queuing models of network systems.

Ning Deng (Senior Member, IEEE) received the B.Eng. degree from the University of Science and Technology of China (USTC) in 2002 and the Ph.D. degree from The Chinese University of Hong Kong (CUHK) in 2007. He is currently a Full Professor with Great Bay University (GBU), China. Prior to GBU, he was a Technology Expert at Huawei and has made multiple contributions to optical switching networks and high-speed transmission systems. He has more than 65 patents granted or pending. He has published about 70 papers in refereed conferences and journals. He is a fellow of Optica (formerly OSA). He was an editor of multiple ITU-T and CCSA standards. He is an Associate Editor of *Journal of Optical Communications and Networking* (JOCN).